



Published in final edited form as:

*Biomed Microdevices*. 2013 February ; 15(1): 37–48. doi:10.1007/s10544-012-9685-0.

## A MEMS Electrochemical Bellows Actuator for Fluid Metering Applications

Roya Sheybani<sup>1</sup>, Heidi Gensler<sup>1</sup>, and Ellis Meng<sup>1,2,3</sup>

<sup>1</sup>Department of Biomedical Engineering, Viterbi School of Engineering University of Southern California, 1042 Downey Way, DRB-140, Los Angeles, CA 90089-1111, USA

<sup>2</sup>Department of Electrical Engineering, Viterbi School of Engineering, University of Southern California, 3651 Watt Way, VHE-602, Los Angeles, CA 90089-0241, USA

### Abstract

We present a high efficiency wireless MEMS electrochemical bellows actuator capable of rapid and repeatable delivery of boluses for fluid metering and drug delivery applications. Nafion®-coated Pt electrodes were combined with Parylene bellows filled with DI water to form the electrolysis-based actuator. The performance of actuators with several bellows configurations was compared for a range of applied currents (1-10 mA). Up to 75 boluses were delivered with an average pumping flow rate of  $114.40 \pm 1.63 \mu\text{L}/\text{min}$ . Recombination of gases into water, an important factor in repeatable and reliable actuation, was studied for uncoated and Nafion®-coated actuators. Real-time pressure measurements were conducted and the effects of temperature, physiological back pressure, and drug viscosity on delivery performance were investigated. Lastly, we present wireless powering of the actuator using a class D inductive powering system that allowed for repeatable delivery with less than 2% variation in flow rate values.

### Keywords

MEMS electrochemical bellows actuators; wireless powering; fluid metering; patient tailored site-specific drug delivery devices

### Introduction

Drug delivery is essential in the treatment and management of chronic conditions such as hypertension, respiratory disease, and diabetes that plague some 125 million Americans (Menehan 2006). However, the most commonly used administration routes, oral or injection, require high systemic doses to achieve the intended therapeutic effect at a remote targeted site within the body. The collateral damage that results from adverse reactions to such high doses motivate the desire to develop implantable site-specific drug delivery systems that minimize side effects, improve safety, and have the potential to be more effective by allowing the use of more potent drugs (Fiering, Mescher et al. 2009). Over the last two decades, microelectromechanical systems (MEMS) micropumps have been developed for broad biomedical and biological applications (Laser and Santiago 2004). A subset of these pumps address requirements for implantable drug delivery systems including biocompatibility, reliable operation (precise and accurate flow control), low power consumption, low heat generation, large driving force, and compatibility with a large variety of new and conventional drugs (Geipel, Goldschmidt et al. 2008; Tang, Smith et al. 2008; Amirouche, Yu et al. 2009). However, the emphasis has been on continuous pumping. New

<sup>3</sup>Corresponding Author: Ellis Meng Phone: (213) 740-6952 Fax: (213) 821-3897, ellis.meng@usc.edu.

evidence in chronotherapy studies point to the therapeutic benefits of the timely delivery of drug, both in terms of duration and time point, within the targeted tissue's therapeutic window (Bruguerolle and Labrecque 2007). Thus, it is clinically relevant to investigate MEMS-based implantable drug delivery technologies that can provide controlled drug volumes at specific times and locations within the body.

Timing and precision of delivery of liquid formulations depend on pump microactuator performance. Thus, selection of actuation methods, dynamic or displacement, are dictated by performance requirements relating to parameters such as flow rate, back pressure, power, efficiency, reliability, and size (Laser and Santiago 2004; Nguyen and Wereley 2006). Dynamic micropumps continuously add energy to the working fluid by directly increasing pressure or momentum; in the latter, conversion into pressure is achieved through an external fluid resistance. Among dynamic actuation methods, magnetohydrodynamic (MHD-DC) actuators are capable of delivering flow rates of up to 1200  $\mu\text{L}/\text{min}$  (Bruguerolle and Labrecque 2007), however, the working fluid must be conductive and the system requires external electric and magnetic fields (Tsai and Sue 2007) that increase power, size, and cost. Displacement micropumps, on the other hand, exert pressure forces on the working fluid using one or more moving boundaries (Laser and Santiago 2004). Electrostatic (Judy, Tamagawa et al. 1991) and piezoelectric (Junwu, Yang et al. 2005) actuators in displacement micropumps are capable of delivering high flow rates ( $>50 \mu\text{L}/\text{min}$ ), and yet are generally larger in size, structurally complex, and require high power (Tsai and Sue 2007). Such actuator types are generally not suitable or difficult to implement *in vivo*.

Electrochemical actuation offers many advantages for displacement micropumps, including large driving force, accurate flow control, low power consumption, and low heat generation (Li, Sheybani et al. 2010). The large volume expansion achieved by electrolysis of water to form oxygen and hydrogen gas can be harnessed for actuation (Tsai and Sue 2007). Current control of electrolysis allows for on-demand activation of delivery and selection of flow rate; the current magnitude and resulting flow rate are linearly correlated for flow control over a wide range of flow rates. Dose volume is selected by pump activation time for a particular flow rate which enables intermittent drug delivery. Electrochemical pumps could have biocompatible construction and wireless actuation (Li, Sheybani et al. 2010) and are well suited for *in vivo* drug delivery applications. In addition, the metering capability of such pumps is also useful for microfluidics and lab-on-a-chip applications.

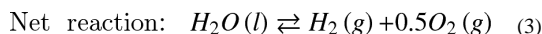
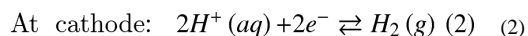
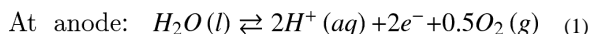
Previously, we reported evaluation of Nafion® -coated electrodes for continuous electrolysis-based pumping coating significantly improved the repeatability and efficiency of current-controlled electrolysis (Sheybani and Meng 2012). Using electrode-only actuators, reliable, precise, and accurate flow control with low power consumption, low heat generation, and large driving force was demonstrated. Here, we present the design, fabrication, and characterization of electrochemical bellows actuators having Nafion®-coated electrodes for controlled intermittent pumping of fluid boluses. Such capability is motivated by unmet needs in chronic drug delivery applications (Fig. 1). The Parylene bellows separates the electrolysis reaction from the pumped drug to prevent unwanted electrochemical or chemical interactions. Electrolysis gases are trapped within the bellows preventing their delivery with the fluid. A new high yield process produced robust bellows consisting of arbitrary numbers of convolutions which were capable of withstanding higher pressures and cycling encountered in high flow rate, rapid bolus delivery (Gensler, Sheybani et al. 2011).

Characterization of actuator flow performance is presented, including characterization during recombination phase (current off) with and without the addition of a commercial

check valve. Real-time pressure measurements for an actuator with a 2 convolution bellows, as well as, the influence of changes in temperature, drug viscosity, and applied back pressure on flow rate and delivery accuracy, are discussed. Finally, a wireless powering system and wireless operation results are described.

## Theory

Water electrolysis is initiated when a sufficient potential or current is applied to a pair of electrodes in contact with an electrolyte (water). The reaction induces water dissociation into oxygen and hydrogen gas. At the anode, oxygen gas, protons, and electrons are produced. The protons are then driven through the electrolyte to the cathode and combine with electrons in the external circuit to form hydrogen gas at twice the rate of oxygen (Bohm, Timmer et al. 2000). A 3:2 stoichiometric ratio conversion of gas to liquid with the standard potential ( $E^\circ$  (25 °C)) of -1.23 V results (Cameron and Freund 2002; Choi, Bessarabov et al. 2004). The reactions at each electrode and the net reaction are summarized in equations 1-3. The theoretical achievable volume expansion from liquid water to gas phase hydrogen at room temperature is 136,000% (Cameron and Freund 2002). This large volume change proceeds even in a pressurized environment making electrolysis an attractive actuation method (Li, Sheybani et al. 2010).



A number of molecular processes influence the rate of gas evolution and the performance of electrolysis actuators. Electrolytically evolved gas first dissolves in the electrolyte adjacent to the electrodes leading to supersaturation of the adjacent electrolyte facilitated by the low solubility and small diffusion coefficient of oxygen and hydrogen gases in water. At low current densities, the dissolved gas remains in the electrolyte (Bohm, Timmer et al. 2000) and is transported to the surrounding bulk electrolyte solely through diffusion, and so supersaturation near the electrodes becomes constant. However, at higher current densities, supersaturation will exceed the threshold required for bubble formation. Bubbles form on the electrode and detach once the Archimedes' force on the bubble exceeds surface adhesion forces (Verhaart, De Jonge et al. 1980; Neagu 1998). Mass transfer of gases controls bubble growth (Shibata 1978) and under constant current conditions, is proportional to the square root of time (Sillen, Barendrecht et al. 1982). Thus, constant current is the preferred mode for electrolysis actuation.

There are no side reactions that could produce undesirable products and potentially reduce the efficiency of gas generation (Neagu, Jansen et al. 2000; Xie, Miao et al. 2004). Gas generation efficiency may be reduced by dissolution of gases into the solution, recombination of gases into water, Joule heating, pressure drop across the actuator membrane, and diffusion of gases through the membrane (Stanczyk, Ilic et al. 2000; Xie, Miao et al. 2004). Efficiency can be improved by increasing current density through methods such as increasing electrochemically active electrode surface area and minimizing occlusion by evolved gases or gas films (Neagu, Jansen et al. 2000).

Over time, the slow diffusion of oxygen through water results in the formation of an "O<sub>2</sub> film" on the electrode surface (Shibata 1978). This film impedes further electrolysis by

preventing liquid-metal contact (Sillen, Barendrecht et al. 1982). Nafion®, a solid polymer electrolyte manufactured by Dupont, was introduced in (Sheybani and Meng 2012) to improve efficiency. Solubility of O<sub>2</sub> and H<sub>2</sub> is 1.8 times higher in Nafion® compared to water (Maruyama, Inaba et al. 1998). This allows for rapid diffusion of gas bubbles away from the surface of the electrodes and prevents occlusion by the gas film. It was reported that Nafion® coated electrodes exhibited a 20% increase in current density (Maruyama, Inaba et al. 1998).

Once the current is removed, gases recombine to form water, however, this reaction is limited by high overpotentials and high activation energy (Broka and Ekdunge 1997; Gensler, Sheybani et al. 2012). Pt can catalyze recombination and is thus commonly selected as the actuator electrode material. In this case, recombination rate is subject to the slow diffusion of O<sub>2</sub> and H<sub>2</sub> to the surface of the Pt electrodes.

## Actuator Operation, Design, and Fabrication

The bellows actuator consists of an electrolyte-filled chamber formed by a Parylene bellows and rigid substrate supporting a pair of interdigitated Pt/Ti electrodes. For pumping applications such as drug delivery, the bellows is coupled to a fluid reservoir. Current application induces electrolysis and the volume expansion inflates the Parylene bellows which expels fluid in the reservoir through an outlet catheter (Fig. 1). Recombination of the gases to water when the current is turned off allows the bellows to return to the original starting position ensuring reliable actuator operation and preventing irreversible damage to the bellows.

A bellows was selected over a corrugated or flat diaphragm for its greater achievable deflections at lower applied pressures (Li, Sheybani et al. 2010). Moreover, additional convolutions are easily added to increase achievable deflection without significantly increasing overall device size (Gensler, Sheybani et al. 2011). Parylene bellows (1, 1.5, and 2 convolutions; 9 mm outer diameter, 6 mm inner diameter) were fabricated as described in (Gensler, Sheybani et al. 2011) and using a new process compared to (Li, Sheybani et al. 2010) (Figs. 2-3). Briefly, 0.4 mm thick silicone rubber sheets (10:1 base-to-curing agent ratio Sylgard 184, Dow Corning, Midland, MI) were punched with 9 and 6 mm holes, aligned, and stacked in alternating layers on glass slides as to form mold modules. These molds were filled with molten (~50°C) polyethylene glycol (PEG; 1,000 Mn, Sigma Aldrich, St. Louis, MO), taking care to ensure that no air bubbles were introduced to the molds. Once PEG solidified at room temperature, silicone molds were peeled away to release the solid PEG modules. The modules were stacked and fused together by slightly moistening interfaces with water. A 13.5 μm layer of Parylene C (Specialty Coatings Systems, Indianapolis, IN) was deposited over the PEG mold, and PEG was dissolved by soaking in water at room temperature to complete the bellows. The number of convolutions were chosen based on previous deflection data (Li, Sheybani et al. 2010; Gensler, Sheybani et al. 2011) and kept low to minimize the overall actuator height.

Interdigitated Pt electrodes (100 μm wide elements separated by 100 μm gaps, 8 mm diameter footprint, 300 Å/2000 Å Ti/Pt) were fabricated on soda lime substrates by liftoff following e-beam deposition of the thin film metal using a previous developed process (Figs. 2-3) (Gensler, Sheybani et al. 2012; Sheybani and Meng 2012). The electrode layout was selected to maximize electrolysis reaction efficiency (Li, Sheybani et al. 2010). Electrodes were potentiostatically cleaned at ±0.5 V (Gamry Reference 600 Potentiostat, Warminster, PA) in 1X phosphate buffered saline. To produce a 1 μm thick coating, Nafion® (Dupont DE521 Solution, Ion Power, INC, New Castle, DE) was applied by dip coating twice. Conductive epoxy (Epo-tek® H20E, Epoxy Technology, Billerica, MA) was

used to affix Kynar™ silver plated copper wires (30 AWG, Jameco Electronics, Belmont, CA) to contact pads on the electrodes. The joint was strengthened and insulated with nonconductive marine epoxy (Loctite, Westlake, OH) (Sheybani and Meng 2012).

To assemble the actuators, bellows were cut to size using a razor blade, filled with DI water, and carefully combined with the Nafion®-coated interdigitated Pt electrodes using laser cut double-sided pressure sensitive adhesive film (3M™ Double Coated Tape 415, 3M, St. Paul, MN). The seal was reinforced with marine epoxy (Loctite, Westlake, OH; Figs. 2-3).

## Experimental Methods

The performance of actuators was systematically characterized. First, actuator performance under continuous pumping conditions at different currents and for each of the three different bellows configurations (1, 1.5, and 2 convolutions) was investigated. The pressure increase during pumping mode was acquired in real time. Recombination mode operation with or without a commercial check valve at the outlet to prevent backflow of fluid during the recombination phase was investigated. Then bolus delivery was assessed for several delivery regimens in which flow rates, bolus volumes, and number of boluses were varied. The study of rapid and repeated bolus mode operation is driven by the potential application of self-administration drug addiction studies in small animals. In this paradigm, doses must be administered immediately (< 5 sec) and repeatedly in response to designated activities to allow the study of correlations between behavior and drug addiction. The impact of environmental factors and fluid composition on pumping were investigated by varying temperature, applied back pressure, and viscosity. Finally, wireless operation of the actuator was demonstrated.

### Pumping Mode Actuator Characterization Under Continuous Operation

The flow rate performance of each bellows configuration under continuous operation was assessed by clamping the actuator within a reservoir formed by an acrylic test fixture filled with double distilled water. Constant current was supplied to the electrolysis electrodes for 2 minutes (Keithley 2400, Keithley Instruments Inc., Cleveland, OH). Flow rate was calculated using the weight of accumulated pumped water. All other experiments were performed with bellows having 2 convolutions to maximize the fluid volume accessible by the actuator for electrolysis.

Real-time measurements of electrolysis chamber pressure were collected at different currents (1, 2, 5, 8, and 10 mA) using a pressure sensor (ASDX015D44R, Honeywell International Inc., Morristown, NJ) connected directly to the outlet of the test fixture. Sensor data was sampled using a data acquisition unit (LabVIEW 9.0.1 with NI cDAQ-9174, National Instruments Corp., Austin, TX). Each current was applied for 90 seconds during which the pressure was measured in real-time.

### Recombination

In order to fully investigate the recombination behavior of the actuator, a large range of volumes of generated gases were required, some of which were beyond the bellows operating range. Therefore, recombination experiments were performed without the Parylene bellows.

Flow rate performance of uncoated and coated electrodes was acquired within an acrylic test fixture filled with double distilled water. The same test fixture was used for all experiments in order to keep the volume of the electrolysis chamber constant. The generated and recombined gas volumes were calculated by measuring water front displacement in a calibrated 100  $\mu$ L micropipette attached to the test fixture outlet. Different volumes of gas

were generated by varying the duration of 10 mA current application. ON/OFF times were equal. Another set of experiments were carried out, in which the volume of gas generated was varied by applying different constant current values (1, 2, 5, 8 mA) for 2 min. Recombination was observed for an hour following each current application.

### **Bolus Delivery**

Actuator performance mimicking conditions necessary for drug self-administration was investigated in three studies. Bolus delivery and recombination were compared in uncoated and Nafion®-coated bellows actuators for rapid-fire delivery of groups of 3 boluses at 10 mA (15 seconds ON, 10 seconds OFF) separated by 5 minute OFF cycles. Forty boluses were delivered at 10 mA (15 seconds ON, 60 seconds OFF). Seventy-five boluses were delivered at 10 mA (2 seconds ON, 60 seconds OFF) using a bellows having a larger outer diameter (10 mm).

While recombination is essential to reliable actuation, it also results in a reverse pressure gradient. Backflow into the pump was prevented by connecting a commercial check valve between the reservoir and the outlet catheter. A Qosina 80031 in-line check-valve with < 0.35 kPa (0.05 psi) cracking pressure, acrylic and ethylene propylene diene monomer construction, and a 3.1-3.43 mm outer diameter (Qosina, Edgewood, NY) was selected. 15 boluses were delivered at 10 mA (15 seconds ON, 60 seconds OFF). Accumulated volume was calculated by measuring water displacement in a 100  $\mu$ L calibrated micropipette.

### **Flow Performance at Body Temperature**

Broka et al. (Broka and Ekdunge 1997) showed that permeability of Nafion® to oxygen and hydrogen increased slightly when ambient temperature was raised from room (25 °C) to body temperature (37 °C). Increased permeability of Nafion® may lead to increased reaction rates and more effective pumping. Temperature effects on flow performance were evaluated using a Nafion®-coated electrode (without bellows) in an acrylic test fixture placed in a constant temperature water bath. Flow rate was calculated by weighing pumped water accumulated over 2 minutes of current application. Then, rapid-fire delivery of 10 boluses at 8 mA (5 seconds ON, 1 min OFF) at room (25  $\pm$  0.2 °C) and body temperatures (37  $\pm$  0.2 °C) were performed on a Nafion®-coated actuator with a 2 convolution bellows. Accumulated volume was calculated by measuring water displacement in 100  $\mu$ L micropipette.

### **Pumping of Viscous Fluids**

The effects of viscosity on flow performance were investigated using three different model drug solutions (propylene glycol, diluted ISOVUE 370, and cocaine). Propylene glycol is a colorless and odorless alcohol compound that has been used as a solvent and a drug carrier in pharmaceutical products (Ooya and Yui 2000; Kogan and Garti 2006; Lee, Oh et al. 2010). ISOVUE 370 is a contrast agent containing iodine used in radiological examinations. Cocaine is a suitable agent for studying drug addiction in a self-administration paradigm in small animals. For propylene glycol, several concentrations were prepared by diluting stock with DI water. ISOVUE 370 (Bracco Diagnostic Inc., Princeton, NJ) was diluted 1:1 with DI water. Cocaine was dissolved in 0.9 N saline. The viscosity of these solutions was measured using a Cannon-Fenske routine viscometer (Technical Glass Products, Painesville Twp., OH) immersed in a water bath at 37 °C.

Model drug solutions were loaded into a polypropylene reservoir containing a Nafion®-coated, 2 convolution bellows actuator. Multiple boluses were delivered (propylene glycol: 10 boluses at 8 mA (10 seconds ON, 60 seconds OFF); ISOVUE 370: 3 boluses at 3 mA (90 seconds ON, 30 minutes OFF); cocaine 3 boluses at 8 mA (60 seconds ON, 15 minutes

OFF)) and the flow rate was calculated from measuring fluid displacement in a 100  $\mu\text{L}$  calibrated micropipette or by weighing the accumulated dispensed fluid.

### Effects of Applied Back Pressure on Flow Performance

During *in vivo* pumping, the actuator must overcome any back pressure associated with the local physiological conditions near the catheter outlet. For instance if the drug is to be delivered in the thoracic vena cava, the backpressure would be equal to the central venous pressure (CVP). The normal range in humans was reported to be approximately  $\sim 3 - 8$  mmHg (Goers 2008). A range of back pressures close to the CVP were applied in order to study their impact on bolus delivery. Four boluses were delivered at 5 mA (60 seconds ON, 120 seconds OFF).

### Wireless Powering System

A 2 MHz class D wireless powering system was developed for wireless operation (Sheybani and Meng 2011) (Fig. 4). Wireless power transfer was performed with concentric placement of the primary ( $\varnothing 55$  mm) and secondary ( $\varnothing 23$  mm) coils and in the same plane ( $0^\circ$  foaveation between coils). Twenty boluses were delivered at 6.3 mA (5 seconds ON, 60 seconds OFF) using an actuator housed in a polypropylene reservoir with 1 mL volume.

## Experimental Results

### Pumping Mode Actuator Characterization Under Continuous Operation

Flow rate is linearly dependent on applied current (Sheybani and Meng 2012). The addition of the drug separating bellows does not affect this relationship. As expected, flow rates were comparable for bellows with different convolutions (Table 1) and not significantly different as confirmed by statistical analysis of the obtained flow rates (ANOVA,  $p < 0.05$ ). The 1 convolution bellows, however, was expanded beyond its elastic operation range at 10 mA current and irreversibly damaged. Actuator operating range is therefore limited by the mechanical performance of the bellows selected.

Nafion® coating increased electrolysis efficiency leading to faster pressure buildup and subsequently higher flow rates. Figure 5 shows the results for real-time pressure measurement of actuators having coated electrodes for different applied current values. As expected from the flow characterization results, the slope was linearly dependent on the applied current ( $R^2 = 0.9976$ ). Slope can be used to estimate pressure generated at a particular instant in time for a given applied current.

### Recombination

Oxygen reduction (recombination) requires a Pt catalyst. For uncoated electrodes, recombination proceeds slowly as it is limited by slow diffusion of gases through water towards the surface of the Pt catalyst (Neagu 1998). Oxygen and hydrogen gases have a higher solubility in Nafion® compared to water (Maruyama, Inaba et al. 1998) ( $\text{O}_2$  solubility is  $7.2 \times 10^{-6}$  mol.cm<sup>-3</sup> in hydrated Nafion® (Ogumi, Takehara et al. 1984) and  $\text{H}_2$  solubility is  $1.4 \times 10^{-6}$  mol.cm<sup>-3</sup> in hydrated Nafion® and  $0.78 \times 10^{-6}$  mol.cm<sup>-3</sup> in water (Maruyama, Inaba et al. 1998)). The higher solubility facilitates diffusion of gases to the electrode surface and may also establish a concentration gradient that further drives diffusion; therefore, recombination is facilitated and increased in Nafion®-coated compared to uncoated electrodes (Fig. 6). When the Parylene bellows are combined with Nafion®-coated electrodes, recombination follows a predictable non-linear diffusion dependent pattern and 99.08% recombination is achieved within one hour of delivery (145  $\mu\text{L}$  delivered volume, data not shown). As expected from the recombination results for electrodes only, gas bubble interactions on the surface of uncoated electrodes and slow

diffusion of gases through water, lead to a random and unpredictable recombination rate. With Nafion® coating, direct bubble interaction with electrodes is avoided. Recombination rate is a function of three factors, transport of gas through water to Nafion®, transport of gas through Nafion® to the electrode, as well as, ratio of gas to liquid inside the bellows.

For Nafion®-coated electrodes, recombination is not directly dependent on applied current or its duration. Rather, it is dependent on the volume of gas generated during the actuation phase. Gas recombination occurs in two phases. The rate is diffusion limited while bubbles are diffusing through the water and Nafion® to the surface of the catalyst but once a sufficient volume of gas bubbles are available at the surface of the catalyst, the recombination becomes reaction limited (Verheij 1997). It is important to note that recombination is also dependent on the volume of the vessel in which electrolysis occurs. The smaller the volume, the shorter the path the gas bubbles need to diffuse to reach the surface of the electrode which facilitates recombination.

### **Bolus Delivery**

When comparing bolus delivery results between coated and uncoated electrodes, differences in both delivery rate as well as recombination are readily observed: the overall pumping efficiency under identical operation conditions is increased and recombination rate is highly dependent on gas to liquid ratio (Fig. 7). An average flow rate of  $78.98 \pm 1.68 \mu\text{L}/\text{min}$  (mean  $\pm$  SE) was calculated for the 40 boluses delivered. As evident in Figure 8, the transition from diffusion limited to reaction limited regimes of recombination occurred after  $\sim 175 \mu\text{L}$  of accumulated volume was delivered and limited further delivery. 75 boluses ( $\sim 3.81 \pm 0.05 \mu\text{L}$  (mean  $\pm$  SE) per bolus) were delivered using the Parylene bellows with the larger outer diameter (10 mm) (Fig 9). The aforementioned recombination regimes are dependent on the size of the bellows and its remaining water content. The transition between the two regimes occurs when a particular gas to liquid ratio threshold is reached. As expected based on previous studies detailed in (Gensler, Sheybani et al. 2011), the bellows having larger diameter achieved higher expansion, therefore, the change in regime would occur at larger volumes that are not reached in Figure 9.

With the bellows actuator connected to the commercial check valve, 15 boluses were delivered with an average bolus volume of  $26.22 \pm 0.18 \mu\text{L}$  per bolus (mean  $\pm$  SE). The cracking pressure of the commercial check valve was reported by the manufacturer to be 0.345 kPa (0.05 psi, 2.6 mmHg). Figure 10 shows that this cracking pressure was adequately exceeded by the actuator. The valve did not increase response time or impede flow compared to when the actuator was operated without a valve. These results correspond to the aforementioned real-time pressure measurements for the bellows actuator. However, as previously reported in (Gensler, Sheybani et al. 2012), this valve is not normally-closed as advertised and requires a finite back pressure for complete sealing. This sealing pressure (measured to be greater than 1.03 kPa) against backward flow was not reached under this condition, leading to significant leakage after the delivery session. It is important to note, that backflow can be prevented with a true normally-closed check valve.

### **Flow Performance at Body Temperature**

Flow rate calculations are summarized in the table below (mean  $\pm$  SE, n=3) for continuous pumping with Nafion®-coated electrode only actuators at room and body temperature (without bellows). A slight increase in flow rate was apparent at 37 °C as expected (Table 2).

The slight increase in flow rate was also observed for rapid-fire boluses delivered using actuators with a 2 convolution bellows. 10 boluses with an average volume of  $15.47 \pm 0.13$



$\mu\text{L}$  and  $16.33 \pm 0.18 \mu\text{L}$  per bolus (mean  $\pm$  SE) were delivered at room ( $25^\circ\text{C}$ ) and body temperature ( $37^\circ\text{C}$ ), respectively. The flow rate differences were significant as determined by t-test for two independent samples with unequal variances ( $p < 0.01$ ).

### Pumping of Viscous Fluids

Despite the large range of viscosities, change in propylene glycol solution flow rate was less than 2.4% (Fig. 11). One way analysis of variance of the data showed that the changes in flow rate for different viscosities were not significantly different compared to one another ( $p < 0.05$ ). Similarly for the ISOVUE 370 dye, an average flow rate of  $30.00 \pm 0.0 \mu\text{L}/\text{min}$  was measured compared to  $29.33 \pm 0.0 \mu\text{L}/\text{min}$  for water (mean  $\pm$  SE). The dye solution was not viscous enough to impede pumping. However, the effects of drug concentration (effectively viscosity) were more apparent in high concentrations of cocaine and flow rate decreased 21% for 25.73 mg/mL cocaine solution (Fig. 12, viscosity could not be measured due to limited sample).

### Effects of Applied Back Pressure on Flow Performance

The change in flow rate across the range of relevant physiological back pressures was less than 5.5% (Fig. 13). One way analysis of variance of the data demonstrated that changes in flow rate across the different back pressure were not significantly different compared to one another ( $p < 0.05$ ).

### Wireless Powering System

Data for wirelessly operated actuators is summarized in Table 3 (Sheybani and Meng 2011). The standard error calculated for different runs at the same set current value was less than 2% which is less than when powered using the constant current source. The average flow rate calculated for the 20 boluses delivered was  $68.4 \pm 1.23 \mu\text{L}/\text{min}$  (mean  $\pm$  SE).

### Discussion

An electrochemical actuator specified for insulin delivery was reported by Suzuki and Kabata in 2005. The system used hydrogen production to deflect a flat silicone membrane to cause actuation and achieved a flow rate of  $13.8 \mu\text{L}/\text{min}$  (Kabata, Suzuki et al. October 31, 2005 - November 3, 2005). However, with this system, repeatable and reliable delivery could not be achieved since the Ag/AgCl electrode depleted over time so that actuator performance was not consistent. Also, the flat silicone membrane had limited deflection and could potentially leak, allowing toxic  $\text{Ag}^+$  in the body. We previously reported an electrochemical bellows actuator capable of delivering flow rates up to  $6.5 \mu\text{L}/\text{min}$  (at 1 mA) but with uncoated electrodes (Li, Sheybani et al. 2010). The pumping efficiency was significantly increased by Nafion® coating of the Pt electrodes (94% for 13 mA compared to 53% for uncoated electrodes) and reliable and repeatable delivery was achieved (Sheybani and Meng 2012). A new high yield process produced robust bellows consisting of arbitrary numbers of convolutions which were capable of withstanding higher pressures and cycling encountered in high flow rate, rapid bolus delivery (Gensler, Sheybani et al. 2011).

The different bellows configurations did not affect the flow rate, however, increasing the number of convolutions increased accessible fluid volume for actuation (Gensler, Sheybani et al. 2011). For the 1 convolution bellows, the electrolyte volume contained is less, therefore as the water to gas ratio becomes smaller, less water is available for further electrolysis. This could lead to increased power consumption (reaching up to 120 mW for 10 mA applied current for the 1 convolution bellows after 1.67 min of actuation).

Recombination, catalyzed by the Pt electrodes when the current is turned off, is an important factor for reliable and repeatable delivery. Nafion®-coated electrodes resulted in a faster and

more predictable pattern of recombination which can in turn be used to tune delivery parameters applied to the actuator to achieve repeatable and reliable delivery and ensure the bellows are not driven beyond their elastic limit.

A truly normally closed check valve is required to prevent backflow of fluids as a result of the reverse pressure gradient caused by recombination. Alternatively, a pressure compensation chamber could be utilized to remedy such complications.

Various environmental factors such as temperature, fluid viscosity, and back pressure could affect actuation flow rate and efficiency. For each application, the environmental factors should be carefully evaluated. Changing the actuation temperature from room temperature (25 °C) to body temperature (37 °C) showed to cause a significant rise in flow rate; this could be attributed to the slight increase in permeability of Nafion® to oxygen and hydrogen when ambient temperature is raised from room (25 °C) to body temperature (37 °C) (Broka and Ekdunge 1997). The actuator is able to pump fluid over a wide range of viscosities, however, for sufficiently high viscosities (> 26 cSt), the flow rate may be affected. A range of applied back pressures within the normal range of CVP in humans (approximately ~ 3 - 8 mmHg (Goers 2008)) did not affect the actuation flow rate significantly.

## Conclusion

We demonstrated the design, fabrication and characterization of a high efficiency electrochemical bellows actuator capable of rapid and repeatable bolus delivery (up to 75 boluses delivered with an average pumping flow rate of  $114.40 \pm 1.63 \mu\text{L}/\text{min}$  in less than 78 minutes) with low power consumption in the mW range (2-25 mW for 1-10 mA applied current). Real-time pressure measurements of the actuator confirm the linear relationship observed between applied current and flow rate. Recombination, essential to accurate and repeatable delivery was studied and it was shown that a predictable pattern can be discerned for Nafion®-coated electrodes. Effects of body temperature, physiological back pressure, and drug viscosity on delivery performance were investigated. Lastly, we presented wireless powering of the actuator using a class D inductive powering system that allowed for repeatable delivery with less than 2% variation in flow rate values. Future work includes, improving wireless system to reduce power requirements and heat dissipation, designing a more suitable check-valve to completely prevent backflow of fluid towards the actuator, and fully packaging the actuator inside a rigid biocompatible polypropylene drug reservoir.

## Acknowledgments

This work was funded in part by a Wallace H. Coulter Foundation Early Career Translational Research Award and NIH/NIDA under award number R21DA026970. The authors would like to thank Drs. D. Holschneider, J.M. Maarek, D. Zhu, and the members of the USC Biomedical Microsystems Laboratory for their assistance with this project.

## References

- Amirouche F, Yu Z, et al. Current micropump technologies and their biomedical applications. *Microsystem Technologies*. 2009; 15(5):647–666.
- Bohm S, Timmer B, et al. Closed-loop controlled electrochemically actuated micro-dosing system. *Journal of Micromechanics and Microengineering*. 2000; 10:498–504. Compendex.
- Broka K, Ekdunge P. Oxygen and hydrogen permeation properties and water uptake of Nafion 117 membrane and recast film for PEM fuel cell. *Journal of Applied Electrochemistry*. 1997; 27:117–123. Copyright 1997, IEE.
- Bruguerolle B, Labrecque G. Rhythmic pattern in pain and their chronotherapy. *Advanced Drug Delivery Reviews*. 2007; 59(9-10):883–895. [PubMed: 17716777]

- Cameron CG, Freund MS. Electrolytic actuators: Alternative, high-performance, material-based devices. *Proceedings of the National Academy of Sciences of the United States of America*. 2002; 99(12):7827–7831. [PubMed: 12060728]
- Choi, P.; Bessarabov, DG., et al. A simple model for solid polymer electrolyte (SPE) water electrolysis. 14th International Conference on Solid State Ionics (SSI-14); 22-27 June 2003; Monterey, CA. 2004.
- Fiering J, Mescher MJ, et al. Local drug delivery with a self-contained, programmable, microfluidic system. *Biomedical Microdevices*. 2009; 11:571–578. Compendex. [PubMed: 19089621]
- Geipel A, Goldschmidt F, et al. An implantable active microport based on a self-priming high-performance two-stage micropump. *Sensors and Actuators A (Physical)*. 2008; 145-146:414–422. Copyright 2008, The Institution of Engineering and Technology.
- Gensler H, Sheybani R, et al. An implantable MEMS micropump system for drug delivery in small animals. *Biomedical Microdevices*. 2012; 14(3):483–496. [PubMed: 22273985]
- Gensler, H.; Sheybani, R., et al. Rapid non-lithography based fabrication process and characterization of Parylene C bellows for applications in MEMS electrochemical actuators. 16th International Solid-State Sensors, Actuators and Microsystems Conference, Transducers '11; Beijing, China. 2011.
- Goers TA. *The Washington Manual of Surgery*, Lippincott Williams & Wilkins. 2008
- Judy, JW.; Tamagawa, T., et al. Surface-machined micromechanical membrane pump. *Proceedings. IEEE Micro Electro Mechanical Systems An Investigation of Micro Structures, Sensors, Actuators, Machines and Robots (Cat No.91CH2957-9)*; 30 Jan.-2 Feb. 1991; New York, NY, USA. 1991.
- Junwu K, Yang Z, et al. Design and test of a high-performance piezoelectric micropump for drug delivery. *Sensors and Actuators A (Physical)*. 2005; 121:156–161. Copyright 2006, IEE.
- Kabata, A.; Suzuki, H., et al. Micro system for injection of insulin and monitoring of glucose concentration. October 31, 2005 - November 3, 2005; Fourth IEEE Conference on Sensors; Irvine, CA, United states.
- Kogan A, Garti N. Microemulsions as transdermal drug delivery vehicles. *Advances in Colloid and Interface Science*. 2006; 123-126:369–385. Compendex. [PubMed: 16843424]
- Laser DJ, Santiago JG. A review of micropumps. *Journal of Micromechanics and Microengineering*. 2004; 14(6):35–64.
- Lee, SH.; Oh, JM., et al. Preparation and characterization of polymeric micelles consisting of poly(propylene glycol) and poly(caprolactone) as a drug carrier. 2010 3rd International Nanoelectronics Conference, INEC 2010; January 3, 2010 - January 8, 2010; Hongkong, China. 2010.
- Li PY, Sheybani R, et al. A parylene bellows electrochemical actuator. *Journal of Microelectromechanical Systems*. 2010; 19:215–228. Copyright 2010, The Institution of Engineering and Technology. [PubMed: 21318081]
- Maruyama J, Inaba M, et al. Influence of Nafion film on the kinetics of anodic hydrogen oxidation. *Journal of Electroanalytical Chemistry*. 1998; 447:201–209. Compendex.
- Menehan, K. National Program Report. M. B. Janet Heroux, Robert Wood Johnson Foundation; 2006. Partnership for Solutions: Better Lives for People with Chronic Conditions.
- Neagu C, Jansen H, et al. The electrolysis of water: an actuation principle for MEMS with a big opportunity. *Mechatronics*. 2000; 10:571–581. Copyright 2000, IEE.
- Neagu, CR. A medical microactuator based on an electrochemical principle. Enschede: Department of Electrical Engineering University of Twente Host; 1998.
- Nguyen, NT.; Wereley, ST. *Fundamentals and applications of microfluidics*. Boston: Artech House; 2006.
- Ogumi Z, Takehara Z, et al. Gas Permeation in SPE Method I. Oxygen Permeation Through Nafion and Neosepta. *Journal of the Electrochemical Society*. 1984; 131(4):769–773.
- Ooya T, Yui N. Supramolecular-structured polymers for drug delivery. *ACS Symposium Series*. 2000; 752:375–384. Compendex.

- Sheybani, R.; Gensler, H., et al. Rapid and repeated bolus drug delivery enabled by high efficiency electrochemical bellows actuators. 5-9 June 2011; 2011 16th International Solid-State Sensors, Actuators and Microsystems Conference, Transducers '11; Beijing, China.
- Sheybani, R.; Gensler, H., et al. Rapid and repeated bolus drug delivery enabled by high efficiency electrochemical bellows actuators. 5-9 June 2011; 16th International Solid-State Sensors, Actuators and Microsystems Conference, Transducers '11; Beijing, China. 2011.
- Sheybani, R.; Meng, E. High efficiency wireless electrochemical actuators: Design, fabrication and characterization by electrochemical impedance spectroscopy. 24th IEEE International Conference on Micro Electro Mechanical Systems, MEMS '11; Cancun, Mexico. 2011.
- Sheybani R, Meng E. High Efficiency MEMS Electrochemical Actuators and Electrochemical Impedance Spectroscopy Characterization. IEEE Journal of Microelectromechanical Systems. 2012
- Shibata S. Supersaturation of oxygen in acidic solution in the vicinity of an oxygen-evolving platinum anode. *Electrochimica Acta*. 1978; 23:619–623. Compendex.
- Sillen CWMP, Barendrecht E, et al. Gas bubble behaviour during water electrolysis. *International Journal of Hydrogen Energy*. 1982; 7:577–587. Copyright 1982, IEE.
- Stanczyk T, Ilic B, et al. Microfabricated electrochemical actuator for large displacements. *Journal of Microelectromechanical Systems*. 2000; 9(3):314–320.
- Tang TB, Smith S, et al. Implementation of wireless power transfer and communications for an implantable ocular drug delivery system. *IET Nanobiotechnology*. 2008; 2(3):72–79. [PubMed: 19045840]
- Tsai NC, Sue CY. Review of MEMS-based drug delivery and dosing systems. *Sensors and Actuators A (Physical)*. 2007; 134(2):555–564.
- Verhaart HFA, De Jonge RM, et al. Growth rate of a gas bubble during electrolysis in supersaturated liquid. *International Journal of Heat and Mass Transfer*. 1980; 23(Copyright 1980, IEE):293–299.
- Verheij LK. Kinetic modelling of the hydrogen-oxygen reaction on Pt(111) at low temperature (170 K). *Surface Science*. 1997; 371(1):100–110.
- Xie J, Miao Y, et al. An Electrochemical Pumping System for On-Chip Gradient Generation. *Analytical Chemistry*. 2004; 76(13):3756–3763. [PubMed: 15228351]

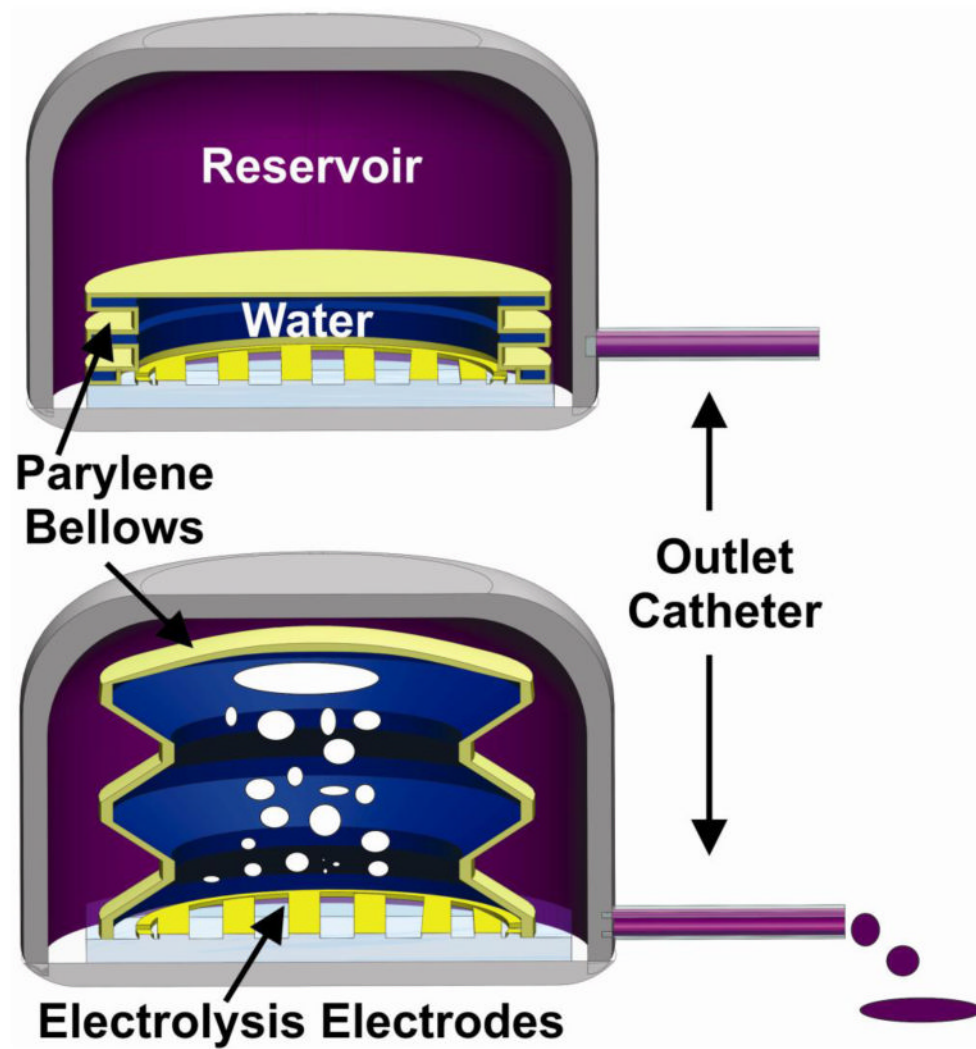


**Figure 1.** Illustration of operation concept of electrochemical bellows actuator. Actuator is shown housed within a reservoir to illustrate the case of fluid metering through an attached catheter.

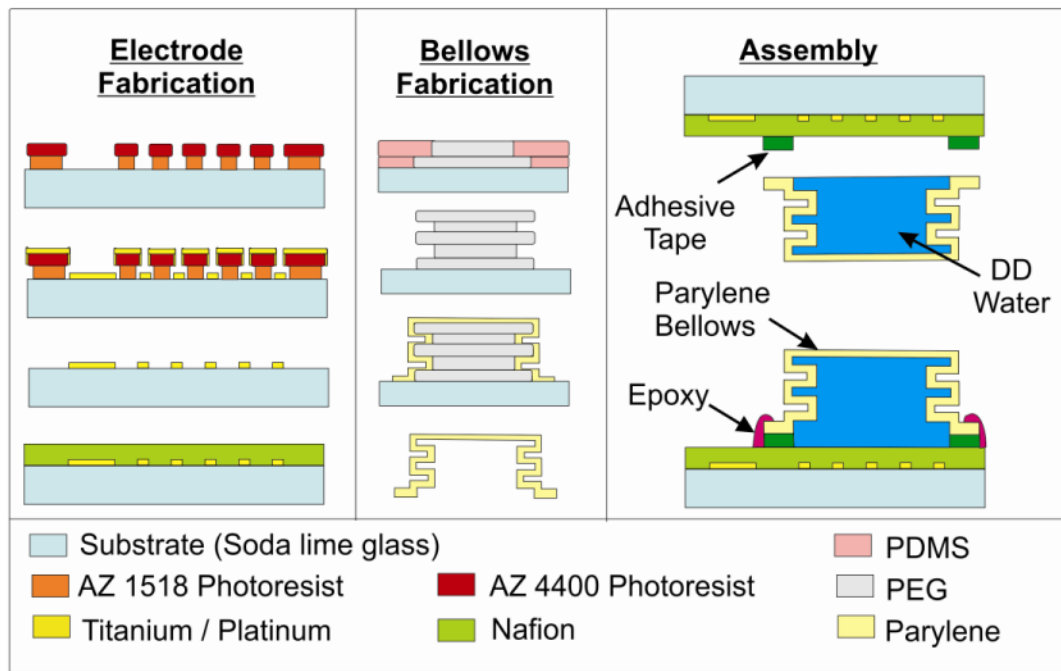


**Figure 2.** Illustration detailing the electrode and bellows fabrication processes and bellows actuator assembly. A 2 convolution bellows is shown.

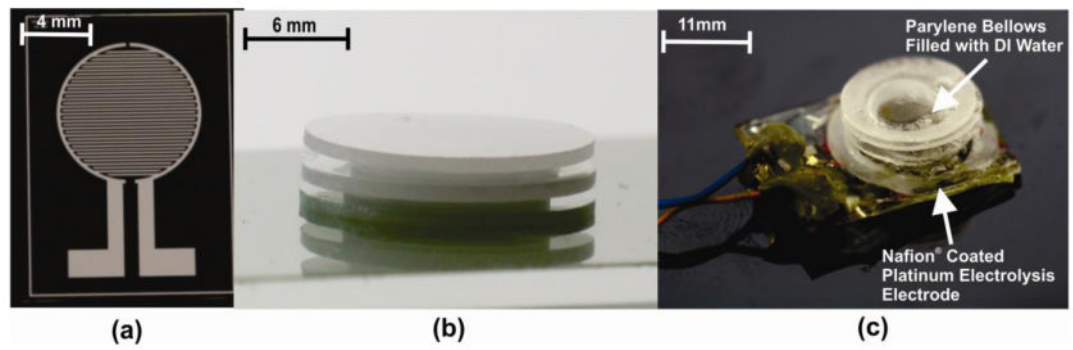


**Figure 3.**  
Photograph of: (a) Pt electrolysis electrode, (b) 2 convolution Parylene bellows, (c) assembled bellows actuator.

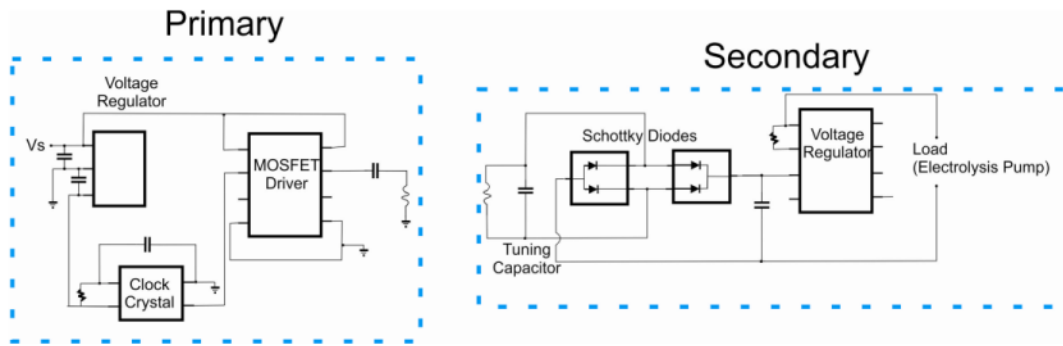


**Figure 4.**  
Circuit schematic for class D wireless inductive powering system.



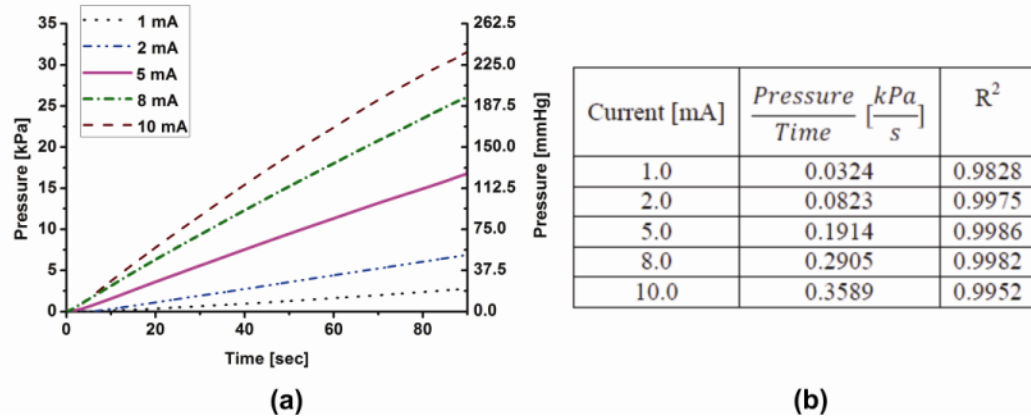


**Figure 5.** (a) Real-time pressure measurements of a 2 convolution Nafion®-coated bellows actuator under constant current application; (b) Slope values for real-time pressure vs. time for different current values.

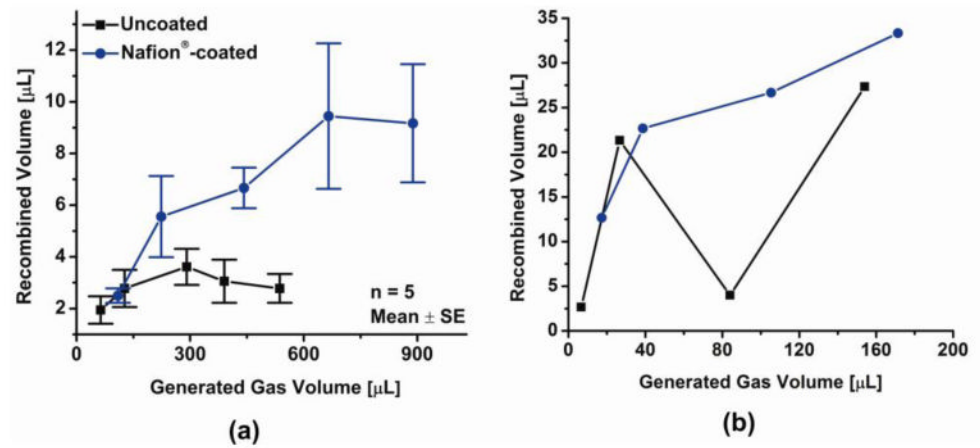


**Figure 6.** Comparison between recombined volume for uncoated and coated electrodes: (a) current controlled (10 mA) delivery for different ON/OFF times (Sheybani, Gensler et al. 5-9 June 2011) and (b) time controlled (2 min) flow rate delivery at different applied currents.

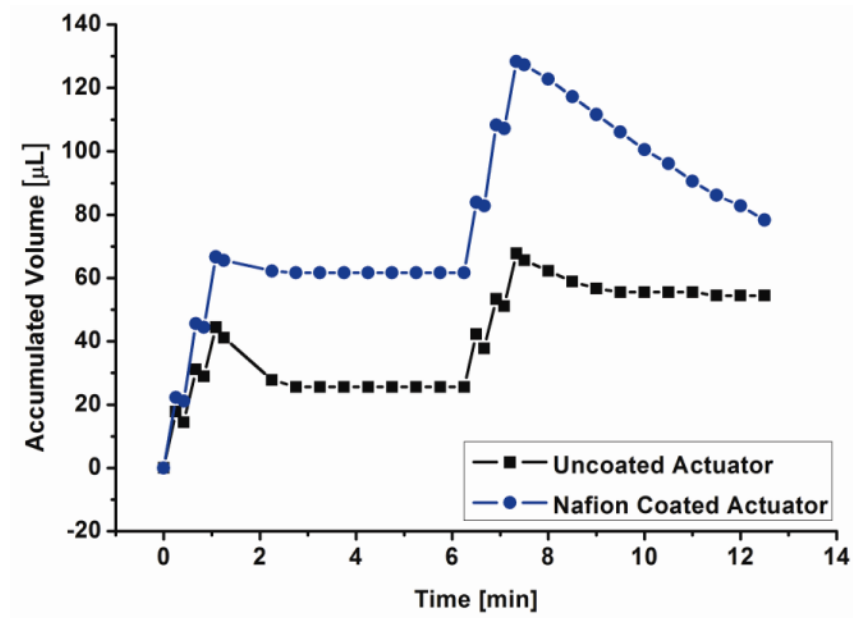


**Figure 7.** Comparison between rapid-fire bolus delivery using uncoated and coated 2 convolution bellows actuators (3 boluses at 10 mA, 15 sec ON/10 sec OFF, separated by 5 min OFF cycles (Sheybani, Gensler et al. 2011)).

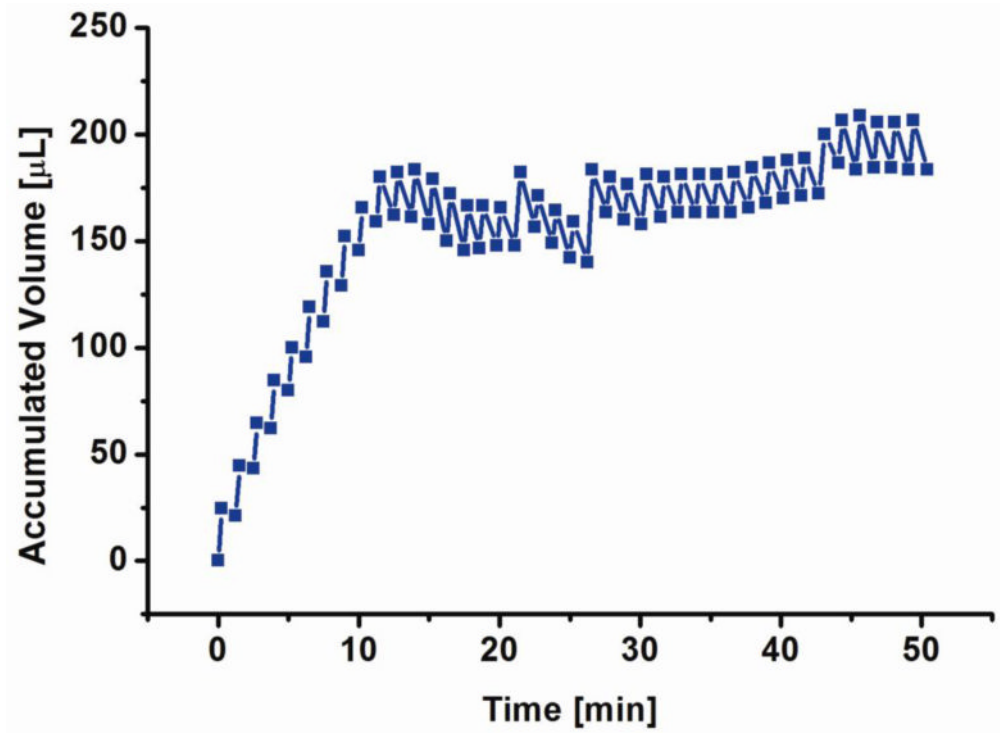


**Figure 8.** Bolus delivery with a Nafion® coated, 2 convolution bellows actuator (at 10 mA current, 15 sec/1 min ON/OFF, modified from (Sheybani, Gensler et al. 2011)).

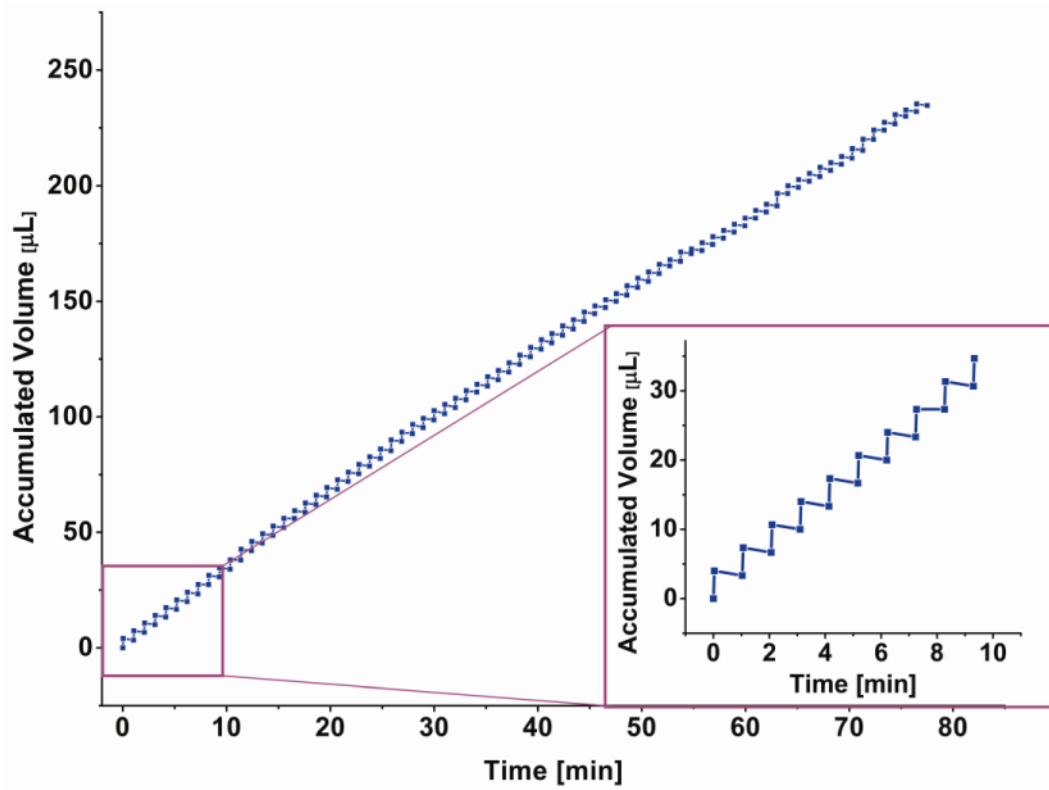


**Figure 9.** Bolus delivery with a Nafion® coated, 2 convolution bellows actuator (at 10mA current, 2 sec/1 min ON/OFF), inset: close-up for first 10 boluses delivered.

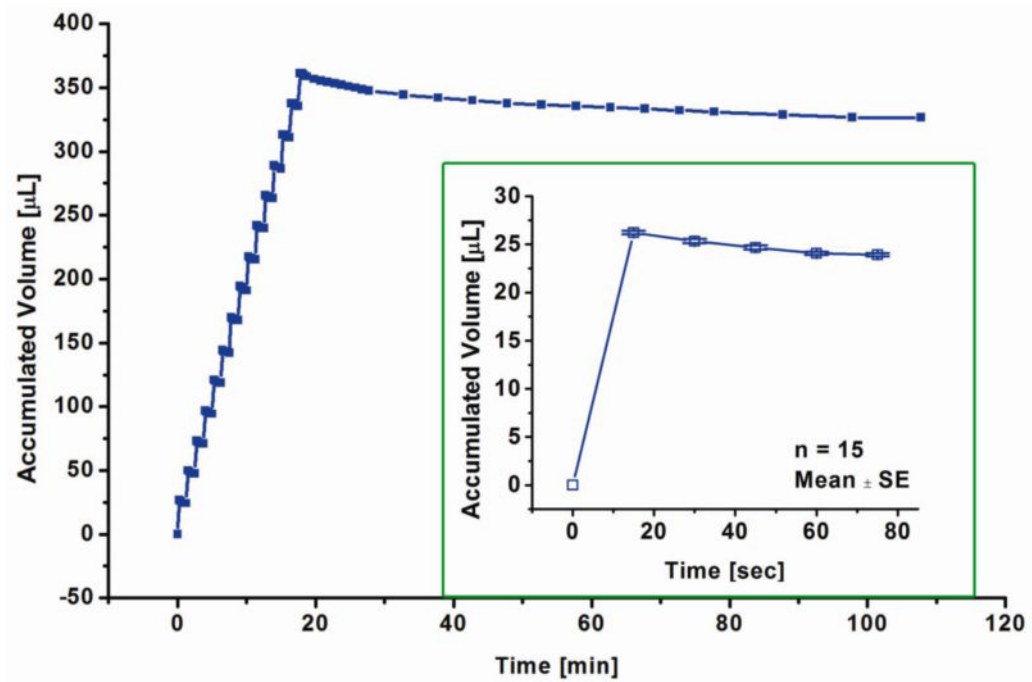


**Figure 10.**

Bolus delivery using an actuator with an in-line check valve (at 10 mA current, 15 sec ON/ 60 sec OFF). After 15 boluses, the actuator is turned off. Inset shows average accumulated volume for 15 boluses.

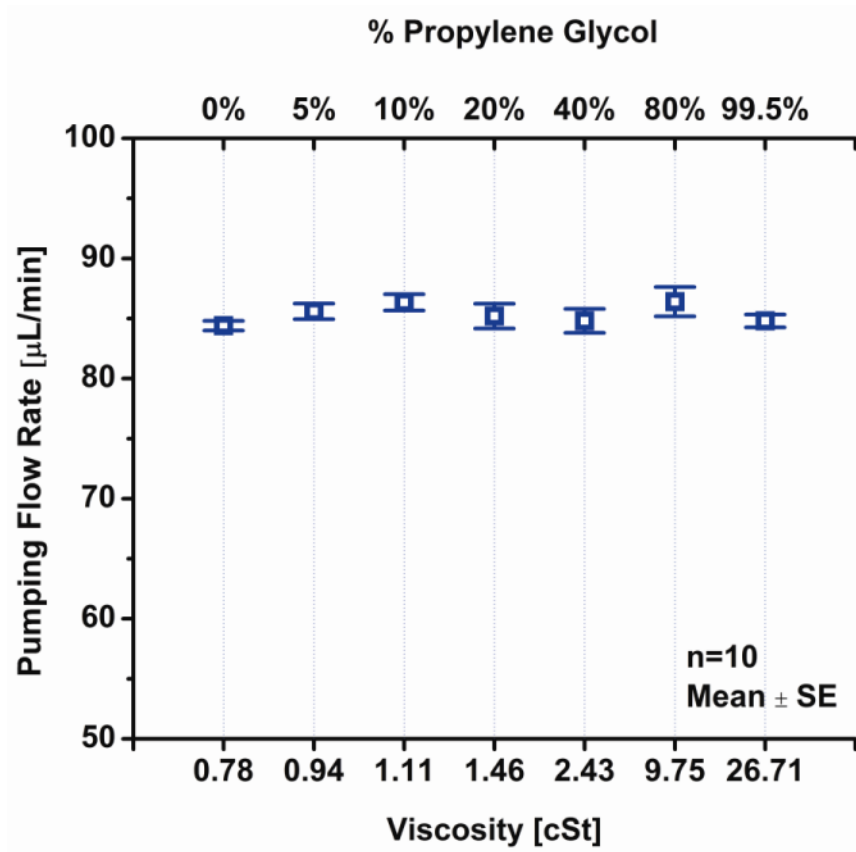


**Figure 11.** Flow delivery results for of different viscosities of propylene glycol (at 8 mA constant current).

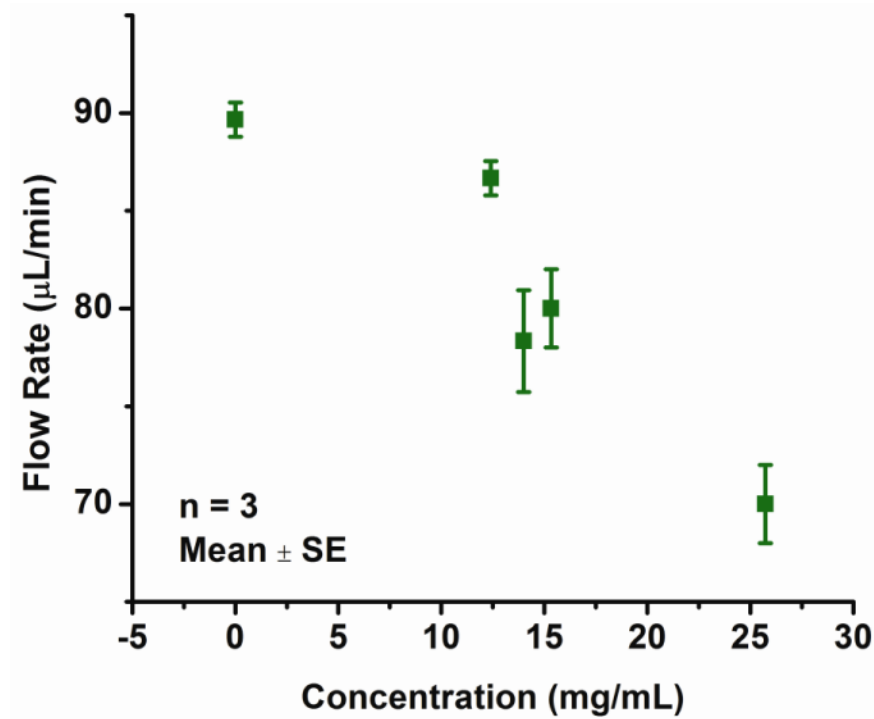


**Figure 12.** Current controlled flow delivery of cocaine (in 0.9 N saline) loaded in a pump at different concentrations (at 8 mA, 1.5 convolution bellows, modified from (Sheybani, Gensler et al. 2011)).



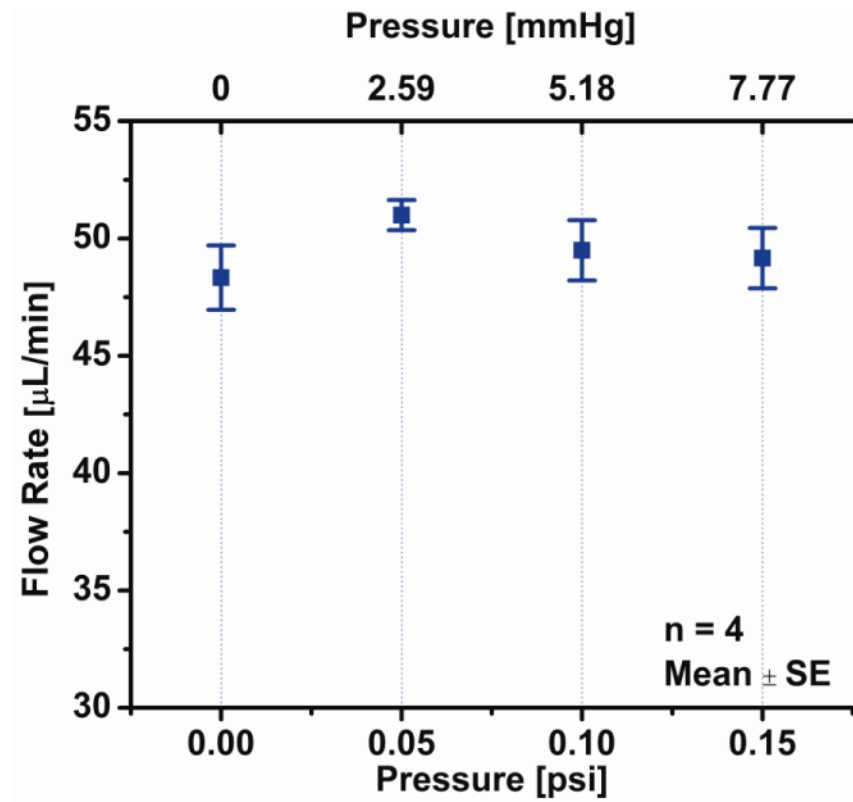


**Figure 13.** Flow delivery results for a range of physiologically relevant back pressures (at 5mA constant current).

**Table 1**  
**Flow rate values for 1, 1.5, and 2 convolutions bellows actuators (Sheybani, Gensler et al. 2011)**

Current [mA]	Flow Rate [ $\mu\text{L}/\text{min}$ ]		
	1 Convolution	1.5 Convolution	2 Convolution
1	$7.33 \pm 0.17$	$9.88 \pm 0.31$	$7.04 \pm 0.29$
2	$17 \pm 0.29$	$19.54 \pm 0.54$	$17.33 \pm 0.44$
5	$44.33 \pm 2.42$	$49.05 \pm 3.05$	$48.17 \pm 0.33$
8	$75.5 \pm 1.80$	$72.44 \pm 5.35$	$73.66 \pm 0.44$
10	N/A	$100.61 \pm 1.11$	$87.33 \pm 0.83$

**Table 2**

Flow rate values for current controlled delivery at room temperature vs. body temperature.

Current [mA]	Flow Rate @ $25 \pm 0.2$ °C [ $\mu\text{L}/\text{min}$ ]	Flow Rate @ $37 \pm 0.2$ °C [ $\mu\text{L}/\text{min}$ ]
1	$8.89 \pm 0.68$	$11.56 \pm 0.47$
2	$21.33 \pm 0.61$	$21.47 \pm 0.50$
5	$54.44 \pm 1.84$	$53.7 \pm 2.96$
8	$89.89 \pm 0.78$	$94.44 \pm 1.15$

**Table 3**

Flow rate values for current supplied using the wireless powering system.

Current [mA]	Flow Rate with Wireless System [ $\mu\text{L}/\text{min}$ ]
2	$20.00 \pm 0.14$
5	$59.00 \pm 1.11$
8	$98.67 \pm 0.41$
10	$125.67 \pm 1.44$